J. Fluid Mech. (1979), *vol.* 92, *part* 2, *pp.* 381–392
Printed in Great Britain

The separation of flow past a cylinder in a rotating system

By LEE-OR MERKINE
Department of Mathematics, Technion–Israel Institute of Technology, Haifa
AND ALEXANDER SOLAN
Department of Mechanical Engineering, Technion–Israel Institute of Technology, Haifa

(Received 21 March 1978)

The flow past a cylinder bounded by parallel planes in a rotating frame is treated in terms of a nonlinear Stewartson layer. It is shown that separation is strongly dependent on the ratio of the Rossby number to the square root of the Ekman number, covering the whole range from fully attached flow to the classical non-rotating separated flow past a cylinder. The results are in agreement with published experimental observations.

1. Introduction

In an experimental study of slightly viscous flow past a circular cylinder in a rapidly rotating frame, Boyer (1970) found a pronounced effect of rotation on the flow field. In the limit of zero Rossby number the flow is fully attached. For finite but small Rossby numbers separation occurs. With increasing Rossby number the point of separation moves away from the rear stagnation point and the angle of separation approaches that of the non-rotating case when the flow is still dominated by rotation, i.e. for Rossby numbers $O(0{\cdot}1)$. The experiments also showed a marked asymmetry of the flow pattern with respect to the undisturbed uniform upstream flow direction. The asymmetry is most pronounced in the wake of the cylinder but it is already observed at the points of separation.

A consideration of strictly two-dimensional rotating flow shows that rotation does not affect separation. This is because in the two-dimensional case no stretching of vortex lines occurs and the vorticity equation is identical to that for the non-rotating case. Therefore the three-dimensionality of the flow field in Boyer's experiments cannot be neglected. This is achieved by accounting for the vortex stretching due to the Ekman suction from the top and bottom horizontal boundary layers. The following analysis shows that Boyer's observations can be interpreted in terms of a nonlinear Stewartson $E^{\frac{1}{4}}$ layer.

2. Analysis

We consider a steady flow past a circular cylinder of radius R and height H bounded by two infinite planes (figure 1). The system rotates with angular velocity Ω parallel to the axis of the cylinder. The flow, unbounded laterally, approaches the cylinder with uniform velocity U.

0022-1120/79/4237-6440 $02.00

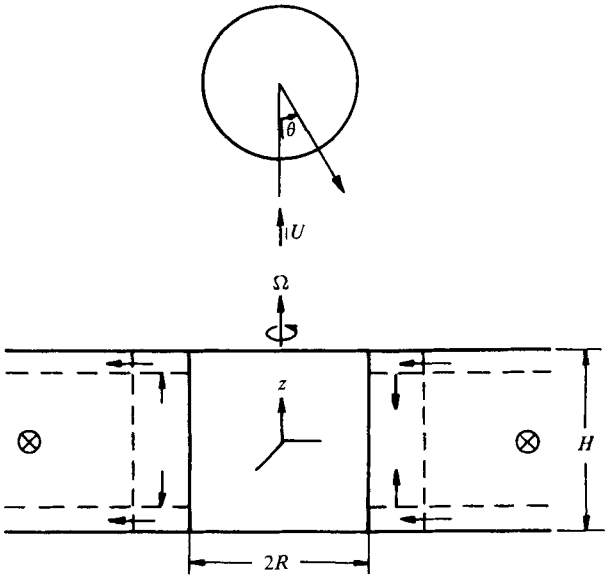

FIGURE 1. Flow geometry.

The non-dimensional equations of motion, in the rotating frame, are

$$Ro(uu_x+vu_y+wu_z) = -\phi_x+v+E_v[u_{zz}+(H/R)^2(u_{xx}+u_{yy})], \tag{1a}$$

$$Ro(uv_x+uv_y+wv_z) = -\phi_y-u+E_v[v_{zz}+(H/R)^2(v_{xx}+v_{yy})], \tag{1b}$$

$$Ro(H/R)^2(uw_x+vw_y+ww_z) = -\phi_z+(H/R)^2E_v[w_{zz}+(H/R)^2(w_{xx}+w_{yy})] \tag{1c}$$

and

$$u_x+v_y+w_z = 0. \tag{1d}$$

Here the scales for (u,v,w) are $(U,U,UH/R)$, the scales for (x,y,z) are (R,R,H), $E_v = \nu/(2\Omega H^2)$ is the vertical Ekman number, $Ro = U/(2\Omega R)$ is the Rossby number, and the pressure field ϕ is measured in units of $2\rho\Omega UR$.

We consider $E_v \ll 1$, $Ro \ll 1$ and $H/R \leqslant O(1)$, such that $Re = Ro/[E_v(H/R)^2] \gg 1$. This divides the flow field into three regions: (*a*) the top and bottom horizontal Ekman layers; (*b*) the vertical boundary layer along the cylinder and (*c*) the interior inviscid flow. Away from the vertical layer, the interior flow is controlled by the secondary circulation imposed by the difference in vorticity between the interior flow and the horizontal boundary layers. This can be expressed in terms of the Ekman suction, which is absent in the interior since the far flow is uniform and has no relative vorticity. The equation governing the stream function of the interior flow is then, to leading order,

$$\nabla^2\psi = 0, \tag{2}$$

with solution

$$\psi = -(r-r^{-1})\sin\theta, \tag{3a}$$

$$u_r = -(1-r^{-2})\cos\theta, \quad u_\theta = (1+r^{-2})\sin\theta, \tag{3b, c}$$

where $r = (x^2+y^2)^{\frac{1}{2}}$.

Unlike the interior flow, vortex stretching is present and is a dominant feature of the flow in the vertical layer. Since there is a difference in vorticity between the

vertical and horizontal layers, Ekman suction occurs and controls the structure of the vertical layer. Apart from this effect, the flow, being rapidly rotating, is quasi-two-dimensional. Thus the equations governing the vertical boundary layer away from the top and bottom layers are

$$Ro(uu_x+vu_y) = -\phi_x+v+E_H u_{yy}, \tag{4a}$$

$$0 = -\phi_y-u, \quad u_x+v_y+w_z = 0. \tag{4b, c}$$

Here $E_H = \nu/(2\Omega R)^2$ is the horizontal Ekman number. Because of the boundary-layer nature of the vertical layer, x and y can be considered as co-ordinates along and normal to the cylinder, respectively. It should be pointed out that the terms $O(Ro)$, which are absent in the quasi-geostrophic approximation, are retained here. This will account for the asymmetry in the relative vorticity, which is of opposite sign on the two sides of the cylinder.

Eliminating u from (4a, c), we obtain

$$Ro(\phi_y\phi_{yx}-v\phi_{yy}) = -\phi_x+v-E_H\phi_{yyy}, \tag{5a}$$

$$-\phi_{yx}+v_y+w_z = 0. \tag{5b}$$

Since the horizontal velocity field is z-independent, (5b) can be integrated from the bottom to the top (i.e. from $z = 0$ to $z = 1$) to yield

$$-\phi_{yx}+v_y+w(1)-w(0) = 0. \tag{6}$$

The vertical velocities $w(0)$ and $w(1)$ at the edges of the horizontal Ekman layers can be related to the difference in vorticity between the vertical layer and the top and bottom planes. (See, for example, Greenspan 1968, p. 106.) Within the framework of the boundary-layer approximation, we can write

$$w(1)-w(0) = -2^{\frac{1}{2}}E_v^{\frac{1}{2}}\phi_{yy}, \tag{7}$$

where we have assumed linear Ekman layers. We now substitute (7) into (6) and integrate with respect to y to obtain

$$v = \phi_x+2^{\frac{1}{2}}E_v^{\frac{1}{2}}\phi_y+f(x), \tag{8}$$

where $f(x)$ is a function of integration, which is determined by substituting (8) into (5a) and using the asymptotic boundary conditions

$$\phi_y \to g(x), \quad \phi_{yy} \to 0, \quad \phi_{yyy} \to 0 \quad \text{as} \quad y \to \pm\infty. \tag{9}$$

The $\pm$ signs here refer to the left and right directions facing downstream. The function $-g(x)$ is the outer flow velocity, determined from the solution of $\nabla^2\psi = 0$. In the present case of flow past a cylinder,

$$g(x) = -2\sin(x). \tag{10}$$

For other configurations $g(x)$ is the appropriate outer flow: for the flat plate, $g(x) = -1$. Consequently

$$f(x) = Ro\,g(g_x-2^{\frac{1}{2}}E_v^{\frac{1}{2}}/Ro) \tag{11}$$

and (5a) takes the form

$$\phi_y\phi_{yx}-\phi_x\phi_{yy}+\frac{E_H}{Ro}\phi_{yyy}-\frac{2^{\frac{1}{2}}E_v^{\frac{1}{2}}}{Ro}\left(-g+\phi_y+\frac{Ro}{2^{\frac{1}{2}}E_v^{\frac{1}{2}}}gg_x\right)(1+Ro\,\phi_{yy}) = 0. \tag{12}$$

At the wall ($y = 0$), $v = 0$, and (8) and (11) yield

$$\phi_x = -f(x), \tag{13}$$

from which we obtain by integration

$$\phi = -\int_0^x dx' f(x') = Ro\left(\int_0^x dx' \frac{2^{\frac{1}{2}} E_v^{\frac{1}{2}}}{Ro} g(x') - \tfrac{1}{2} g^2(x)\right). \tag{14}$$

The no-slip boundary condition at the wall is supplemented by the equation

$$\phi_y = 0 \quad \text{on} \quad y = 0, \tag{15}$$

which is obtained from (4*b*). The structure of the vertical boundary layer is thus given by (12) with the conditions (9), (14) and (15).

It is interesting to examine the various limits.

(*a*) When $Ro \to 0$ and $E_v^{\frac{1}{2}}/Ro \to 0$, we obtain the classical non-rotating boundary-layer equation. This is so because the dissipation of vorticity due to Ekman suction is negligible compared with advection.

(*b*) When $Ro \to 0$ and $E_v^{\frac{1}{2}}/Ro \to \infty$, we obtain the classical linear Stewartson $E^{\frac{1}{4}}$ layer: $E_H^{\frac{1}{2}} H/(2^{\frac{1}{2}} R)\, \phi_{yyy} - \phi_y = -g$.

(*c*) When $Ro \to 0$ we obtain the familiar quasi-geostrophic approximation, i.e. isobars parallel to streamlines.

Equation (12) is parabolic and its integration starts at the forward stagnation point $x = 0$. The integration over each side of the cylinder (left and right relative to the flow direction) is done separately, y extending from zero to plus or minus infinity, respectively. If in the solution for the right-hand side ϕ and y are replaced by $-\phi$ and $-y$, the net effect is to change the term $1 + Ro\,\phi_{yy}$ to $1 - Ro\,\phi_{yy}$, thereby introducing asymmetry. Recall that the term $Ro\,\phi_{yy}$ is the relative vorticity induced in the vertical boundary layer. This term, being $O(Ro)$, is absent in the quasi-geostrophic approximation $Ro \to 0$.

The above analysis indicates that the vertical boundary layer is controlled by the parameters $E_v^{\frac{1}{2}}/Ro$; Ro and H/R. $E_v^{\frac{1}{2}}/Ro$ determines the extent to which the vertical boundary layer is influenced by the horizontal Ekman layers. The effect of asymmetry is introduced through small but *finite* values of Ro.

3. Results and discussion

Equation (12) was solved numerically subject to the boundary conditions (9), (14) and (15) using techniques that have been developed for boundary-layer equations in non-rotating systems (Cebeci, Smith & Wang 1969). Solutions were found for a wide range of Ro, but for $E_v = 4{\cdot}3 \times 10^{-4}$ in order to facilitate comparison with Boyer's experiments.

The dependence of the shear stress along the cylinder and consequently the point of separation on the parameters of the problem is of major physical interest. A *necessary* condition for the existence of separation is the presence of an adverse pressure gradient along the wall. (The actual value of the angle of separation is determined by the vanishing of the shear stress at the wall.) From (13) and (11) it is readily seen that a sufficient condition for the existence of a fully attached flow is that

$$E_v^{\frac{1}{2}}/2^{\frac{1}{2}} R_0 \geqslant 1. \tag{16}$$

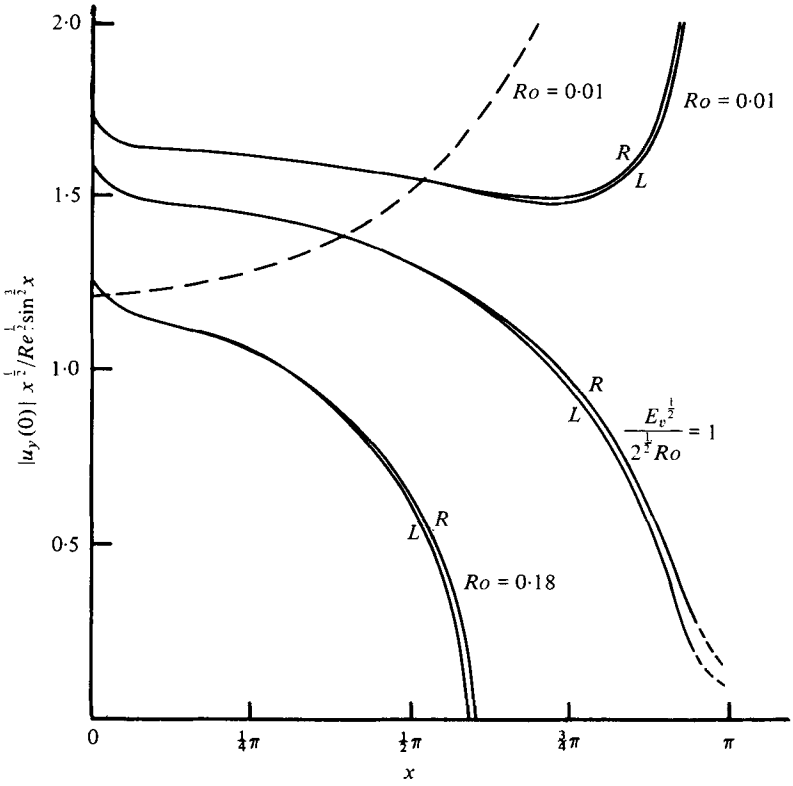

FIGURE 2. Shear stress along the cylinder. $E_v = 4{\cdot}3 \times 10^{-4}$. ——, present theory; – – –, Stewartson's linear solution; L, left side, facing downstream; R, right side, facing downstream.

A necessary condition for the existence of separation is the violation of (16). The physical meaning of (16) is that the slowing down of the advection of vorticity, which is $O(Ro)$, as the flow approaches the rear stagnation point is not necessarily accompanied by a reduced shear stress at the wall since the excess vorticity produced at the wall can be removed through an $O(E_v^{\frac{1}{2}})$ suction of vorticity into the horizontal Ekman layers.

Figure 2 depicts the non-dimensional shear stress along the wall on the two sides of the cylinder for three values of Ro. Note that, besides a minor error due to numerical difficulties in the vicinity of the rear stagnation point, the equality in (16) provides the bifurcation line separating fully attached flows from separated flows. The right–left asymmetry present in the flow field is indicated by a small but systematic increase in the shear stress along the right-hand side of the cylinder (facing downstream) relative to the left-hand side of the cylinder. The mechanism of asymmetry will be explained later when we consider the secondary circulation. The classical linear Stewartson $E^{\frac{1}{4}}$ layer yields

$$|U_y(0)| = -g\frac{R}{H}\left(\frac{2}{E_v}\right)^{\frac{1}{4}} \tag{17}$$

as the non-dimensional shear stress. Figure 2 indicates that even when $Ro = 0{\cdot}01$ and $E_v^{\frac{1}{2}}/Ro \simeq 2{\cdot}07$, such that vortex stretching plays a dominant role in the dynamics

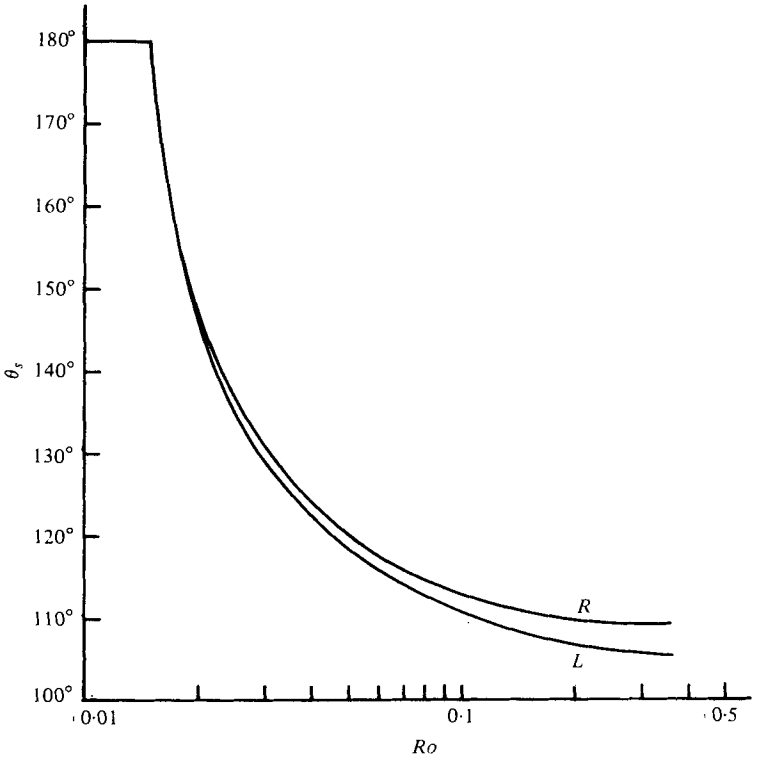

FIGURE 3. Separation angle as a function of the Rossby number. $E_v = 4{\cdot}3 \times 10^{-4}$.

of the vertical boundary layer, the linear theory is unsatisfactory except for $x \simeq \frac{1}{2}\pi$, for which the inviscid solution exterior to the boundary layer is locally stationary on the large scale R.

The dependence of the separation angle θ_s on Ro is shown in figure 3. Note the rapid decrease of θ_s from the value π, corresponding to a fully attached flow, to approximately 109°, which is the angle of separation of the corresponding classical non-rotating two-dimensional flow. Following the usual practice we disregard the effect of the detached flow on the flow field upstream of the separation point. Boyer in his experiments reports that for his value $Ro = 0{\cdot}01$, which corresponds to $Ro = 0{\cdot}02$ in our case [in his paper the Rossby number is defined as $U/(4\Omega R)$], the flow was fully attached. Our results indicate that for $E_v = 4{\cdot}3 \times 10^{-4}$ separation should occur for $Ro > 0{\cdot}0147$ and that for $Ro = 0{\cdot}02$, $\theta_s \simeq 147°$. This discrepancy can be attributed to the fact that near the bifurcation value the results are very sensitive to small changes in Ro, as can be seen from figures 2 and 3. Thus experimental uncertainty in the value of Ro can lead to a different bifurcation value of Ro. Coutanceau & Bouard (1977) report that in the classical non-rotating two-dimensional flow past a right circular cylinder separation occurs first for $Re \simeq 2{\cdot}2$. (Their reported value of 4·4 is based on the diameter, while ours is based on the radius.) If we express (16) in terms of Re we find that separation is initiated when

$$Re = (2E_v)^{-\frac{1}{2}}(R/H)^2. \tag{18}$$

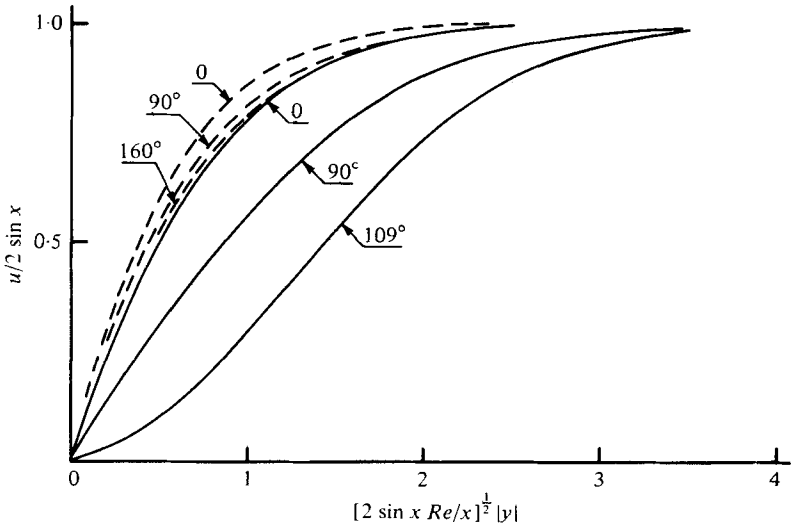

FIGURE 4. Streamwise velocity profiles at various stations along the cylinder. $E_v = 4{\cdot}3 \times 10^{-4}$. All curves for right side of cylinder. ——, $Ro = 0{\cdot}18$; – – –, $Ro = 0{\cdot}01$.

Consequently, in rapidly rotating systems the flow can remain fully attached for Reynolds numbers which are much larger than the critical Reynolds number for the corresponding non-rotating flows. In Boyer's experiments $E_v = 4{\cdot}3 \times 10^{-4}$ and $R/H = 0{\cdot}5$, which yields $Re = 8{\cdot}5$.

Profiles of u at various stations around the cylinder for two values of Ro are shown in figure 4. Note that for $Ro = 0{\cdot}18$ the velocity profile changes markedly with θ, developing an inflexion point as the separation angle is approached. For $Ro = 0{\cdot}01$ the flow field is fully attached and the profile of u changes little in the streamwise direction. The u profiles are shown only for the right-hand side of the cylinder. The u profiles on the left-hand side of the cylinder have the same qualitative appearance.

It was stated earlier that the location of the angle of separation depends on the ability of the horizontal Ekman layers to remove the vorticity produced at the wall since the adverse pressure gradient slows down the mechanism of vorticity advection. If $E_v^{\frac{1}{2}}/Ro < O(1)$ the Ekman layers play a secondary role. Thus when advection of vorticity weakens, the balance in the vorticity equation is achieved by reducing the vorticity produced at the wall. In other words, the shear stress at the wall is reduced and separation occurs closer to the forward stagnation point.

More insight into the mechanism responsible for separation and for the asymmetric properties of the flow field can be obtained if we inspect the secondary circulation, i.e. the velocity field normal to the wall. This is provided in figures 5(*a*) and (*b*), where v *is positive when pointing to the left.* Before inspecting these figures let us make the following observation. The relative vorticity induced in the vertical layers is negative on the left-hand side of the cylinder and positive on the right-hand side. Consequently, the horizontal Ekman layers cause $\partial w/\partial z > 0$ on the left side and $\partial w/\partial z < 0$ on the right side, which in turn leads to a *tendency for* $v < 0$ *on both sides of the cylinder.* This v field advects vorticity towards the wall on the left side and away from the wall on

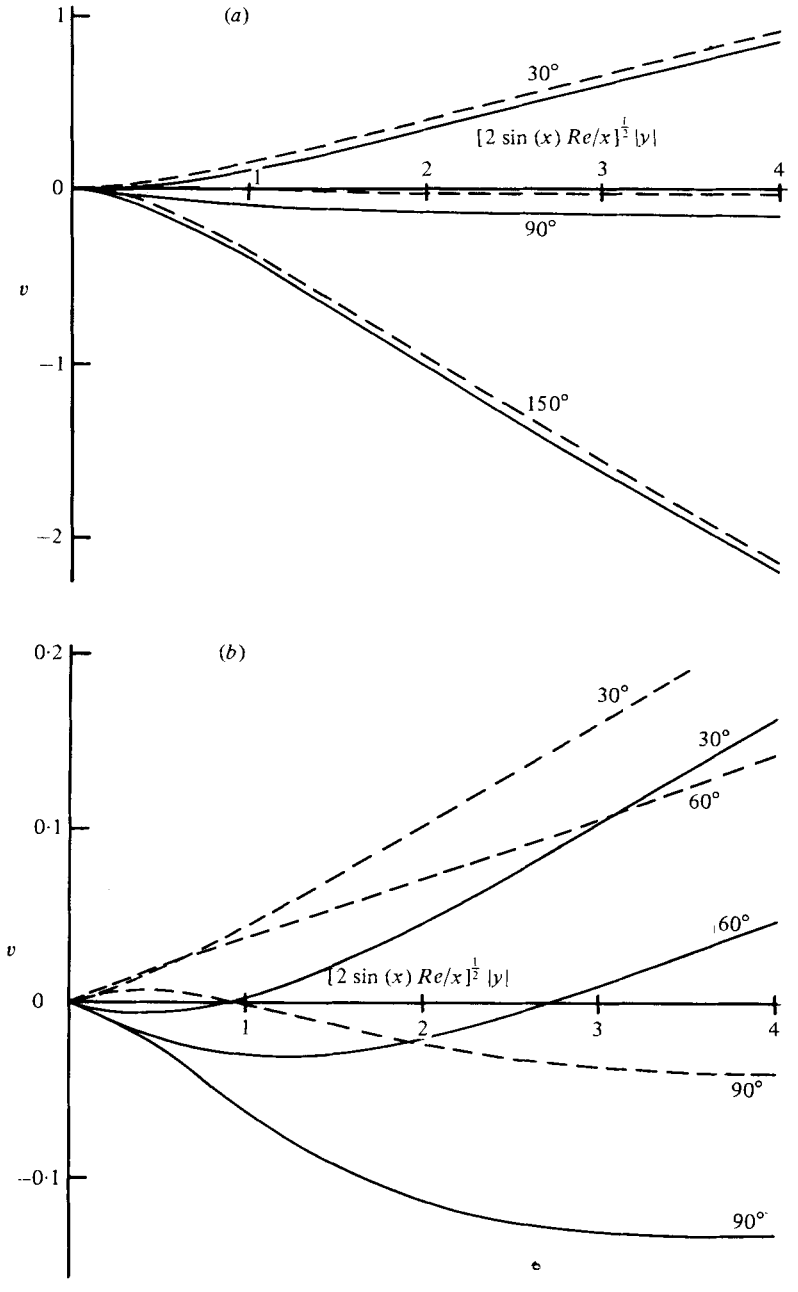

FIGURE 5. Transverse velocity profiles at various stations along the cylinder. $E_v = 4{\cdot}3 \times 10^{-4}$. ——, right side; – – –, left side, velocity shown with sign changed. (*a*) $Ro = 0{\cdot}01$. (*b*) $Ro = 0{\cdot}18$.

the right side. This asymmetry in advection is partially balanced by an asymmetry in vorticity production: the production on the left side is somewhat less than that on the right side. This results in a reduced shear stress on the left side relative to the shear stress on the right side (see figure 3), thus explaining the asymmetry in the location of the separation angle (see figure 3) in accord with Boyer's experimental results.

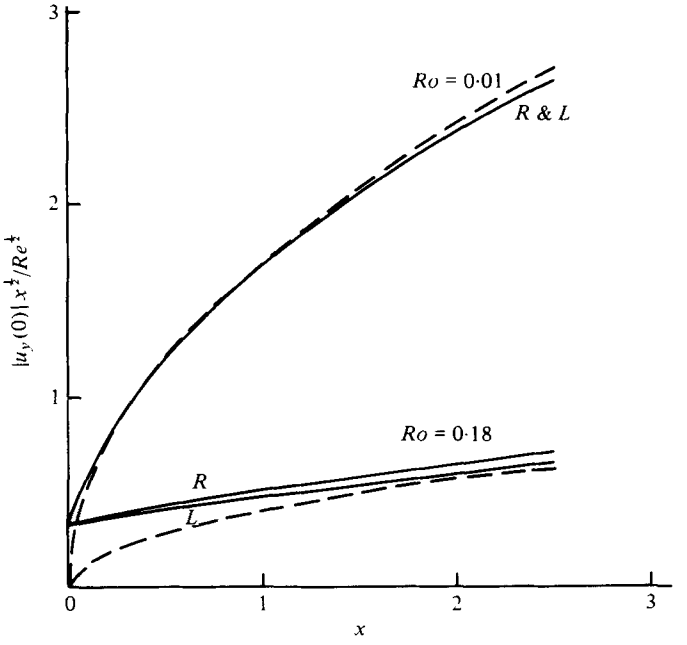

FIGURE 6. Shear stress along flat plate. $E_v = 4{\cdot}3 \times 10^{-4}$. ——, present theory; – – –, Stewartson's linear solution.

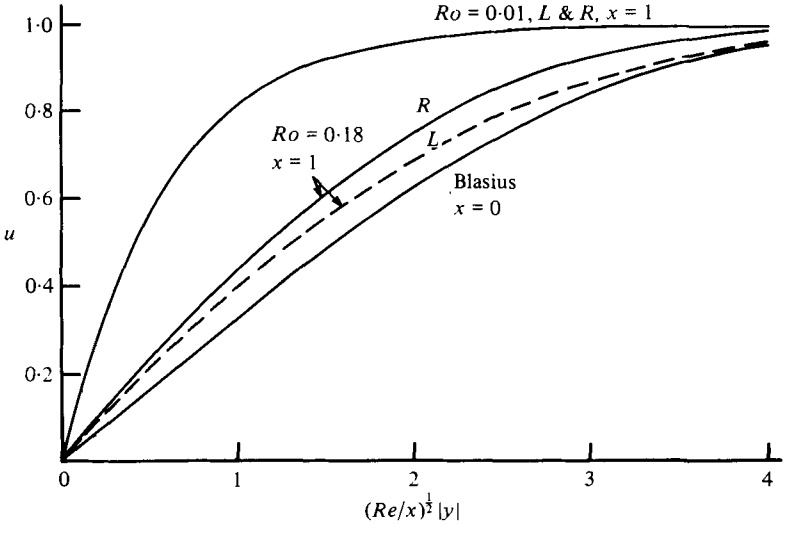

FIGURE 7. Streamwise velocity profiles at various stations along flat plate. $E_v = 4{\cdot}3 \times 10^{-4}$.

The phenomenon of asymmetry is revealed in figures 5 (*a*) and (*b*), and being $O(Ro)$, becomes more pronounced as the Rossby number increases. These figures demonstrate the complex nature of the vertical layer, which has a multiple structure. The inner region is seen to be controlled by the Ekman layer, as discussed above, and $E_v^{\frac{1}{2}}/Ro > O(1)$ locally. In the outer region the influence of the Ekman layers weakens and $E_v^{\frac{1}{2}}/Ro < O(1)$ locally. In the outer region the v field is more in line with the corresponding classical

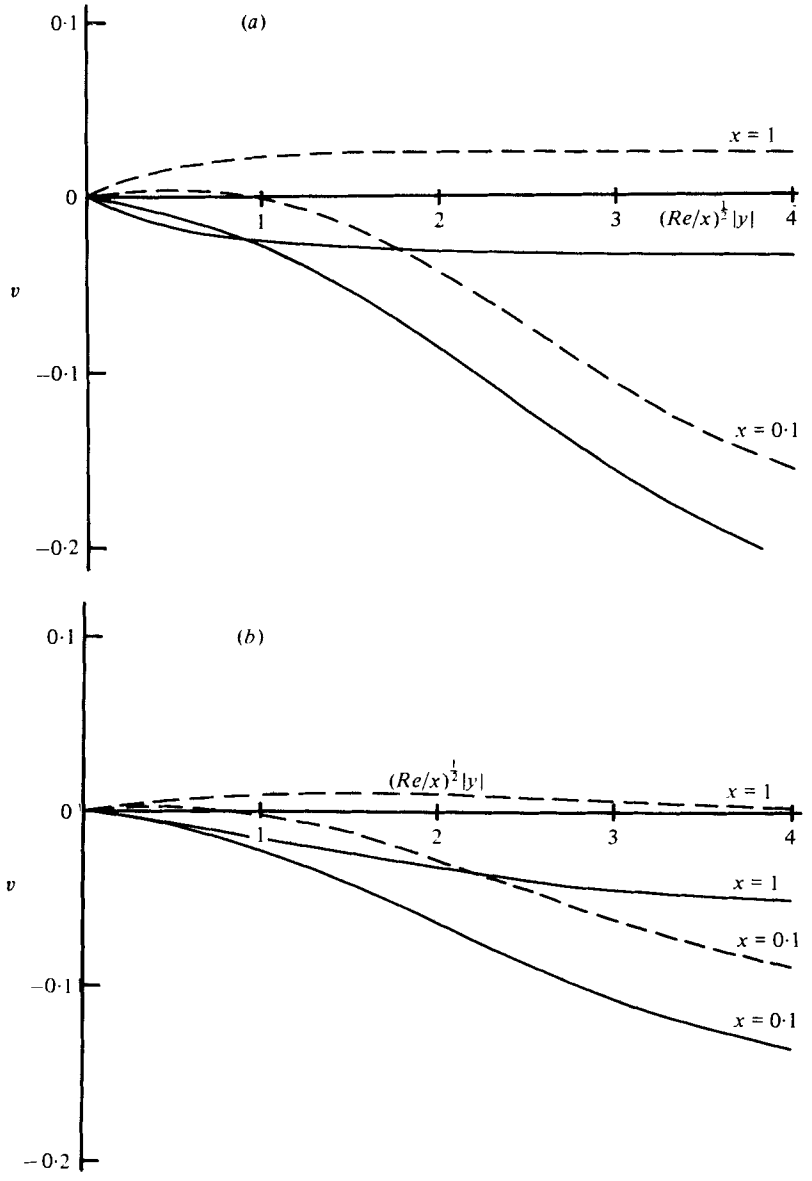

FIGURE 8. Transverse velocity profiles at various stations along flat plate. $E_v = 4{\cdot}3 \times 10^{-4}$. ——, right side; – – –, left side, velocity shown with sign changed. (*a*) $Ro = 0{\cdot}01$. (*b*) $Ro = 0{\cdot}18$.

non-rotating case. The streamwise dependence of the v field follows from the dependence of the inviscid flow at the outer edge of the boundary layer on the streamwise co-ordinate [see (10)]. [Since $E_v^{\frac{1}{2}}/Ro < O(1)$ in the outer region of the boundary layer the continuity equation takes on the approximate form $u_x + v_y \simeq 0$.]

So far we have analysed the flow field past a cylinder in a rotating system. Another problem of interest is that of a rotating flow past a vertical flat plate, for which $g = -1$. The numerical results are depicted in figures 6–8 for the parameter values employed in the case of the cylinder.

Figure 6 shows the non-dimensional shear stress along the wall. The following observations should be made. All solutions yield the same value of shear stress at $x = 0$, i.e.

$$\lim_{x \to 0} x^{\frac{1}{2}} U_y(0, x)/Re = 0{\cdot}332,$$

which is identical to Blasius' solution for the classical two-dimensional non-rotating flow past a flat plate (Schlichting 1968, p. 128). Furthermore, it can be demonstrated that at $x = 0$ the equation governing the boundary-layer structure is identical to Blasius' equation. Consequently, near the leading edge the flow field is always dominated by inertia and advection of vorticity is much more important than the removal of vorticity through the Ekman-layer suction. The situation is reversed downstream and the flow field approaches Stewartson's $E_v^{\frac{1}{4}}$ linear solution, given by (17). The length of the transition region from Blasius' solution to Stewartson's solution increases with Ro. It is astonishing that Stewartson's solution, which has been found totally inadequate for the case of the cylinder, is very satisfactory for the flat plate, provided that we are sufficiently far downstream from the leading edge. The only similarity with the case of the cylinder is that the shear stress develops asymmetry as Ro increases. The sense of the asymmetry is identical to that exhibited in the case of the cylinder.

The features associated with figure 6 are also present in figure 7, which presents profiles of u at the stations $x = 0$ and $x = 1$. The multiple structure of the vertical boundary layer is again demonstrated most easily through the secondary circulation of the v field as shown in figures 8 (a) and (b). The interpretation of the results follows the lines presented for the case of the cylinder. The transition from Blasius' solution to Stewartson's linear solution is most apparent in figure 8 (a), where $v < 0$ at $x = 1$ on both sides of the flat plate. This behaviour, which is completely at odds with the case of the cylinder, is a consequence of u being constant outside the vertical boundary layer.

Finally, it is interesting to note that the results of this study may have geophysical applications. It has been suggested by J. G. Charney (private communication) that vortex shedding resulting from flow separation of a slightly viscous flow past a curved wall might be a possible mechanism for mountain-induced cyclogenesis. Such a situation could be relevant for the case of the Alps, for which a northerly flow passing between the Alps and the Pyrenees might shed large-scale vortices to the western Mediterranean. Such large-scale atmospheric flows are typically characterized by $Ro/E_v^{\frac{1}{4}} > O(1)$, which indicates that the present theory might be applicable.

The authors acknowledge the help of Mrs G. Fruchter, who performed the numerical calculations. This research was supported by a grant from the United States–Israel Binational Science Foundation (BSF), Jerusalem, Israel.

REFERENCES

BOYER, D. L. 1970 Flow past a right circular cylinder in a rotating frame. *J. Basic Engng* **92**, 430–436.

CEBECI, T., SMITH, A. M. O. & WANG, L. C. 1969 A finite-difference method for calculating compressible laminar and turbulent boundary layers. *McDonnell Douglas Rep.* DAC-67131.

COUTANCEAU, M. & BOUARD, R. 1977 Experimental determination of the main features of the viscous flow in the wake of a circular cylinder in uniform translation. Part 1. Steady flow. *J. Fluid Mech.* **79**, 231–256.

GREENSPAN, H. P. 1968 *The Theory of Rotating Fluids.* Cambridge University Press.

SCHLICHTING, H. 1968 *Boundary Layer Theory*, 6th ed. McGraw-Hill.